American Journal of Polymer Science and Technology
2024; Vol. 10, No. 1, pp. 1-14
https://doi.org/10.11648/j.ajpst.20241001.11

Research Article

Bioinspired Nanotubular Structures by Soft-Template Electropolymerization: 3,4-(2,3-naphtylenedioxy)Thiophene Monomers Quenched to Form Dimers

Fatoumata Sow[1], Salif Sow[1], Abdoulaye Dramé[1, *], Alioune Diouf[1], Aboubacary Sene[1], Frédéric Guittard[2], Thierry Darmanin[2]

[1]Laboratory of Organic and Bio-organic Chemistry, Faculty of Science and Technology, Cheikh Anta Diop University, Dakar-Fann, Sénégal

[2]NICE-Lab of the Chemistry Institute, Côte d'Azur University, Nice, France

Abstract

Preparing well-ordered nanotubes on materials surface is a great of interest in many applications. Bio-inspired and theoretical approaches show that porous structures such as nanotubes are key parameters for both surface hydrophobicity and water adhesion. Here, a very easy soft-template electropolymerization approach is used to form nanotubular structures, followed by a bioinspired strategy to control the wetting properties. Fully conjugated monomers based on 3,4-(2,3- naphtylenedioxy)thiophene (NaphDOT) core grafted with many rigid aromatic groups such as phenyl, naphthalene, pyrene, pyrrole, were synthesized. Then, electropolymerization is carried out with these monomers, followed by surface and morphologies characterization of corresponding polymers. We show that even if just dimers are formed by electropolymerization, the resulting polymer can be sufficiently insoluble to form structured films. 3,4-(2,3-naphtylenedioxy)thiophene (NaphDOT) is chosen as a judicious example, due to strong π-stacking interactions, and also their capacity to form nanotubular structures by soft template-electropolymerization in the presence of water (H_2O). Here, different substituents, polymerizable or not, are grafted on the 2-position of thiophene. Films are formed with all the studied substituents. Nanotubular structures are especially observed with the following substituents: hydroxyl, pyrene and pyrrole, but in the presence of H_2O. We study also their influence on the surface hydrophobicity.

Keywords

Nanostructures, Nanotubes, Electrochemistry, Wettability, Hydrophobicity

1. Introduction

The bioinspiration is a fascinating to make a breakthrough in a specific field [1-5]. This is particularly true in the wetting field [6-11]. For example, controlling both the surface energy and the surface structures at a micro and/or nanoscale can induce a huge increase in surface hydrophobicity [12, 13]. The air fraction of rough surfaces being very important as demonstrated by Cassie-Baxter [14], nanotubes were found to be excellent candidates to tune surface hydrophobicity and

*Corresponding author: abdoulay.drame@ucad.edu.sn (Abdoulaye Dramé)

Received: 16 March 2024; **Accepted:** 3 April 2024; **Published:** 17 April 2024

water adhesion, due to their specific aspect ratio [15-17].

Among the processes for preparing rough surfaces, the electropolymerization has various advantages including the rapidity to implement and the control of surface structures [18]. To obtain porous structures such as nanotubes by electropolymerization, one of the strategies is for inducing the polymer growth around a template [19-21]. It was reported in the literature this possibility using hard templates such as anodized aluminium oxide (AAO) membranes. However, this process is long, multi-step and one membrane is necessary for each variation in the nanotube dimension. This is why processes of templateless or soft-template electropolymerization were recently developed. These processes are possible if soft objects including gas bubbles or micelles are present around a substrate. The case of the electropolymerization of pyrrole directly in H_2O has been particularly studied [22, 23]. During electropolymerization and depending on the electropolymerization method, different gases (dioxygen O_2 and hydrogen H_2) can be generated *in-situ* from H_2O, and leading to various nanotubular structures. However, most of the monomers being not soluble in H_2O, this strategy has been also envisaged in organic solvents such dichloromethane (CH_2Cl_2) or chloroform ($CHCl_3$) [22-28]. Particularly, 3,4-(2,3-naphtylenedioxy)thiophene (NaphDOT) was demonstrated as a model molecule leading to vertically aligned nanotubes with high hydrophobicity and water adhesion [29, 30]. Moreover, it was also demonstrated that this monomer can form micelles in solvents of low water solubility (CH_2Cl_2 or $CHCl_3$, for example) as soon as trace H_2O are present in solution [30].

Previously, we demonstrated using NaphDOT that even if one substituent is positioned in polymerization position (2-position) leading to dimers, the resulting polymer can be sufficiently insoluble to form deposit and use in soft-template electropolymerization [31]. This is mainly due to the strong π-stacking interactions. Here, we want to confirm these preliminary results by designing other NaphDOT derivatives (Scheme 1). We want also to show the influence of the electropolymerizable substituent in the used potential range (naphthalene, pyrene, thiophene, pyrrole, and carbazole) compared to non-electropolymerizable substituents (hydroxyl, phenyl, and phenoxyphenyl). The electropolymerizations were performed in CH_2Cl_2 and CH_2Cl_2 saturated with H_2O (CH_2Cl_2 + H_2O sat.).

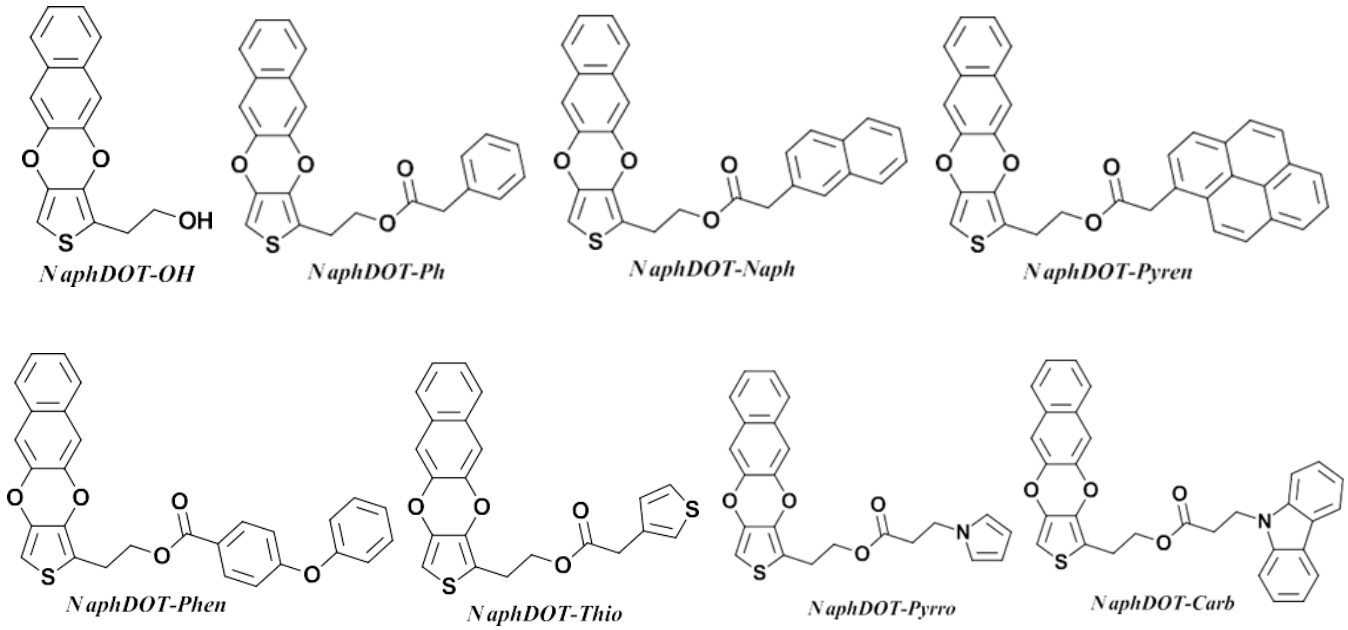

Scheme 1. *Original monomers studied in this manuscript.*

2. Experimental Section

2.1. Monomer Synthesis

The monomers were synthesized in five steps from 3,4-dibromothiophene, as described in Scheme 2.

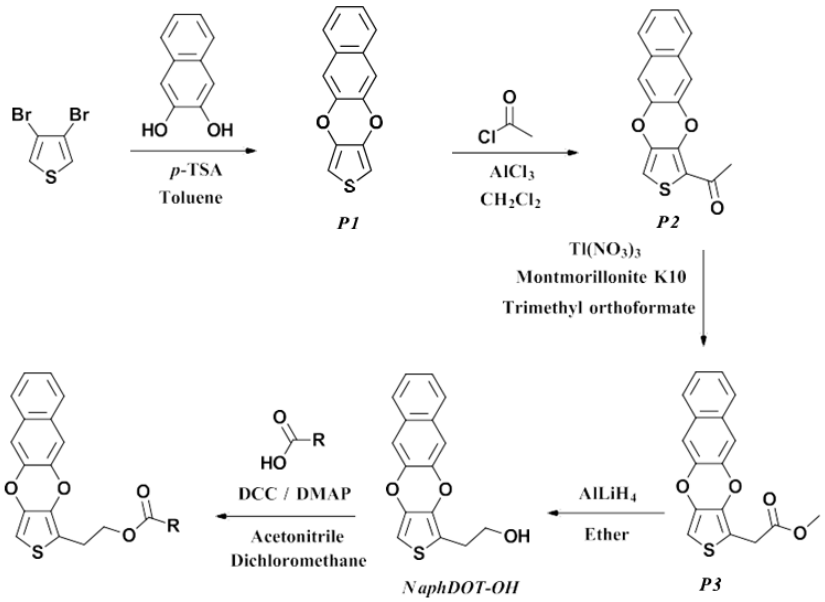

Scheme 2. *Chemical way to the monomers.*

Naphtho[2,3-b]thieno[3,4-e][1,4]dioxine (P1) was synthesized as reported in literature [32]. Synthesis of 1-(naphtho[2,3-b]thieno[3,4-e][1,4]dioxin-7-yl)ethanone (P2):

Aluminum chloride (2.0 g, 15.1 mmol, 1.5 eq) in 55 mL of anhydrous CH2Cl2 was added under argon to NaphDOT (2.4 g, 10.1 mmol, 1 eq) in 200 mL of anhydrous dichloromethane. The mixture was cooled and acetyl chloride (1.60 g, 20.5 mmol, 2 eq) was added dropwise into it under argon flow. The mixture was then stirred at room temperature for a night. Then, hydrochloric acid (50 mL, 1M) was added to quench to solution and the mixture was washed with CH_2Cl_2, dried on Na_2SO_4 and the solvent evaporated. The product (2) was purified by column chromatography (silica gel; eluent: CH_2Cl_2).

Yield: 63%; Dark brown solid; δH(200 MHz, $CDCl_3$): 7.70 (2H, m), 7.40 (4H, m), 6.83 (1H, s), 2.69 (3H, s); δC(50 MHz, CDCl3): 189.11, 140.72, 139.56, 139.43, 138.55, 130.93, 130.37, 126.98, 126.91, 126.00, 125.77, 120.94, 113.21, 112.83, 108.45, 29.31.

Synthesis of methyl 2-(naphtho[2,3-*b*]thieno[3,4-*e*][1,4]dioxin-7-yl)acetate (P3) [33]:

Thallium (III) nitrate (3.1 g, 7.0 mmol, 1.2 eq) was stirred with trimethoxymethane (7.7g, 72.7 mmol, 12.3 eq) in methanol (10 mL) for 5 min. Montmorillonite K10 (6.6 g) was added and the mixture was stirred for 10 min. The solvent was evaporated, P2 (1.7 g, 6.6 mol, 1 eq) was added in 200 mL of methanol/dichloromethane (1:1). The mixture was stirred at room temperature for 2 days. The product was then purified by column chromatography (silica gel; eluent: CH_2Cl_2).

Yield: 37.2%; Beige solid; δH(200 MHz, CDCl3): 7.68 (2H, m), 7.35 (4H, m), 6.44 (1H, s), 3.80 (2H, s), 3.77 (3H, s); δC(50 MHz, $CDCl_3$): 169.59, 140.35, 140.16, 137.98, 137.55, 130.57, 130.40, 126.83, 125.52, 125.46, 112.98, 112.90, 112.67, 101.54, 52.70, 31.04.

Synthesis of 2-(naphtho[2,3-b]thieno[3,4-e][1,4]dioxin-7-yl)ethanol (NaphDOT-OH):

To obtain the corresponding alcohol, the ester function was reduced with LiAlH4 in anhydrous diethyl ether for 1 day and then by performing a basic hydrolysis (4 mg of NaOH in 200 ml of distilled water). The product was then purified by column chromatography (silica gel; eluent: CH2Cl2).

Yield: 75%; White powder, T°f = 126.6°C; δH(200 MHz, DMSO-d6): 7.77 (dd, J = 6.27 Hz, J = 3.30 Hz, 2H), 7.57 (d, J = 5.7 Hz, 2H), 7.39 (m, 2H), 6.82 (s, 1H), 3.64 (t, J = 6.5 Hz,2H), 3.36 (s, 1H), 2.86 (t, J = 6.5 Hz, 2H); δC(200 MHz, DMSO-d6): 145.20, 145.15, 142.37, 139.46, 135.33, 135.29, 131.98, 130.63, 121.76, 117.75, 117.62, 104.09, 65.81, 34.29.

Synthesis of the other monomers:

The corresponding acid (1.2 eq) was mixed with dicyclohexylcarbodiimide (DCC) (138 mg, 1.2 eq) and a catalytic amount of 4-(dimethylamino)pyridine (DMAP) in absolute acetonitrile (20 mL). After stirring for 30 min, 1.0 eq. of NaphDOT-OH was added to this mixture. The mixture was stirred at room temperature for 24 h. After a night, the solvents were totally evaporated and the crude product was purified by silica gel column (eluent CH_2Cl_2: cyclohexane with proportions depending on the monomer).

2-(naphtho[2,3-b]thieno[3,4-e][1,4]dioxin-7-yl)ethyl 2-phenylacetate: Yield: 95 %; yellow powder, T ℉ =72.6 ℃; δH(400 MHz, $CDCl_3$): 7.65 (m, 2H), 7.34 (dd, J= 3.24Hz, J = 6.3 Hz, 2H), 7.30 (m, 3H), 7.27 (d, 1.0Hz, 1H), 7.22 (m, 1H), 7.15 (d, J = 1.5 Hz, 1H), 7.13 (s, 1H), 6.34 (s, 1H), 4.33 (t, J = 6.6 Hz,2H), 3.64 (s, 2H), 3.07 (t, J=6.6 Hz, 2H); δC(400 MHz,$CDCl_3$): 170.39, 139.51, 137.19, 134.59, 132.96, 132.79, 129.41, 128.48, 127.69, 127.51, 126.06, 125.76, 124.28,

113.14, 111.58, 111.49, 97.15, 62.78, 40.35, 24.41.

2-(naphtho[2,3-b]thieno[3,4-e][1,4]dioxin-7-yl)ethyl 2-naphtalenacetate: Yield: 79 %; T ℉ = 89.5 ℃, White powder; δH(400 MHz, $CDCl_3$): 7.74 (m, 4H), 7.68 (s, 1H), 7.62 (m, 2H), 7.40 (m, 2H), 7.26 (d, J = 2.2 Hz, 2H), 7.23 (s, 1H), 7.28 (s, 1H), 6.34 (s, 1H), 4.34 (t, J = 6.6 Hz, 2H), 3.78 (s, 2H), 3.05 (t, J = 6.6 Hz, 2H); δC(400 MHz,$CDCl_3$): 170.36, 139.49, 137.17, 134.6, 132.37 132.42, 130.26, 129.40, 127.39, 127.32, 127.17, 127, 126.66, 126.59, 126.48, 126.31, 125.76, 125.21, 125.06, 124.85, 124.71, 124.25, 111.55, 97.11, 62.81, 40.55, 24.43.

2-(naphtho[2,3-b]thieno[3,4-e][1,4]dioxin-7-yl)ethyl 2-pyrenacetate: Yield: 95 %; T ℉ = 151.5 ℃, Yellow powder; δH(400 MHz, $CDCl_3$): 8.19 (s, 1H), 8.14 (m, 1H), 8.1 (d, J = 1.4 Hz, 2H), 8.06 (d, J = 1.4 Hz, 1H), 8.02 (d, J = 2.0 Hz, 2H), 7.99 (d, J = 1.3 Hz, 1H), 7.95 (d, J= 1.0 Hz, 2H), 7.9 (m, 2H), 7.57 (m, 2H), 7.32 (m, 2H), 7.13 (d, J = 5.1 Hz, 2H), 6.12 (s, 1H), 4.41 (t, J = 6.36Hz, 2H), 4.37 (s, 2H), 3 (t, J = 6.4 Hz, 2H); δC(400 MHz,$CDCl_3$): 171.44, 140.25, 137.99, 131.22, 130.77, 130.32, 129.41, 128.35, 127.86, 127.29, 127.018, 126.75, 126, 125.88, 125.18, 125.05, 124.88, 124.64, 123.17, 113.97, 112.37, 97.91, 63.77, 39.63, 25.44.

2-(naphtho[2,3-b]thieno[3,4-e][1,4]dioxin-7-yl)ethylcarbazole: Yield: 99 % T ℉ = 135.9 ℃; White powder; δH(400 MHz, $CDCl_3$): 7.93 (d, J = 1.0 Hz, 1H), 7.89 (d, J = 1.0 Hz, 1H), 7.49 (m, 2H), 7.26 (m, 4H), 7.15 (m, 4H), 7.05 (m, 2H), 6.15 (s, 1H), 4.48 (t, J = 7.1 Hz, 2H), 4.11 (t, J= 6.6 Hz,2H), 2.81 (t, J= 6.6 Hz, 2H), 2.72 (t, J=7.4 Hz, 2H); δC(400 MHz,$CDCl_3$): 171.23, 140.53, 140.50, 139.96, 138.24, 135.62, 130.47, 126.81, 125.81, 125.36, 123.11, 120.43, 119.23, 113.97, 112.61, 108.57, 98.26, 63.87, 38.7, 33.56, 25.3;

2-(naphtho[2,3-b]thieno[3,4-e][1,4]dioxin-7-yl)ethyl 2-thiophenacetate: Yield: 86 % T ℉ = 60.5 ℃; White powder; δH(400 MHz, $CDCl_3$): 7.65 (m, 2H), 7.34 (dd, J = 3.2 Hz, J = 6.3 Hz, 2H), 7.30 (m, 3H), 7.27 (d, 1.0Hz, 1H), 7.22 (m, 1H), 7.15 (d, J = 1.5 Hz, 1H), 7.13 (s, 1H), 6.34 (s, 1H), 4.33 (t, J = 6.6 Hz,2H), 3.64 (s, 2H), 3.07 (t, J = 6.6 Hz, 2H); δC(400 MHz,$CDCl_3$): 169.91, 139.51, 137.22, 134.63, 132.58, 132.34, 129.42, 127.47, 125.78, 124.97, 124.67, 124.3, 122.06, 121.93, 113.13, 111.58, 97.18, 62.84, 42.38, 34.83, 24.43.

2-(naphtho[2,3-b]thieno[3,4-e][1,4]dioxin-7-yl)ethyl phenoxyphenylacetate: Yield: 55 %; T°f = 98.8°C; δH(200 MHz, $CDCl_3$): 7.97 (dd, J= 6.9 Hz, J= 2.1 Hz, 2H), 7.54 (m, 2H), 7.30 (m, 3H), 7.22 (m, 4H), 7.11 (m, 2H), 6.87 (m, 4H), 6.27 (s, 1H), 4.44 (t, J = 6.3 Hz, 2H), 3.11 (t, J = 6.3 Hz, 2H); δC(200 MHz,CDCl3): 161.97, 140.5, 131.86, 130.42, 130.02, 126.8, 125.33, 124.54, 124.31, 120.19,117.17, 114.51, 112.58, 112.51, 98.22, 64.07, 25.68.

2-(naphtho[2,3-b]thieno[3,4-e][1,4]dioxin-7-yl)ethyl 2-pyrrolate: Yield: 68 %; T°f = 109.8°C; δH(400 MHz, $CDCl_3$): 7.68 (dd, J= 3.29Hz, J = 6.2 Hz, 2H), 7.36 (m, 4H), 6.64 (t, J = 2.1 Hz, 2H), 6.37 (s, 1H), 6.12 (t, J =Hz, 2H), 4.34 (t, J = 6.6 Hz,2H), 4.21 (t, J = 7.0 Hz, 2H), 3.07 (t, J= 6.58Hz,2H), 2.81 (t, J = 7.0 Hz, 2H); δC(400 MHz,$CDCl_3$): 169.84, 139.51, 137.27, 134.65, 129.44, 125.77, 124.33, 119.5, 112.97, 111.58, 111.55, 107.45, 97.23, 62.81, 43.77, 35.55, 24.39.

2.2. Soft-Template Electropolymerization

Here, in order to study the influence of H_2O in soft-template electropolymerization, two solvents were used: CH_2Cl_2 and CH_2Cl_2 saturated with H_2O (CH_2Cl_2 + H_2O sat.). CH_2Cl_2 + H_2O sat. was very easily prepared by mixing CH_2Cl_2 with H_2O and after discarding the aqueous phase. The electrodepositions were performed with an Autolab potentiostat (Metrohm). Gold-coated silicon wafer was used as the working electrode, a carbon rod as the counter-electrode, a saturated calomel electrode (SCE) as the reference electrode. In the solvent, were added the monomer (0.01 M) and the electrolyte (0.1 M of tetrabutylammonium perchlorate). After determining the monomer oxidation potentials ($E^{ox} \approx 2$ V vs SCE) by 1) cyclic voltammetry, the electrodepositions were performed using two processes: by cyclic voltammetry (E = -1 V to E^{ox}) with a scan rate of 10 mV s^{-1} and different number of scans, and 2) at constant potential (E = E^{ox}) with different charges.

2.3. Surface Characterization

The surface structures were explored by scanning electron microscopy (SEM). The surface roughness by optical profilometry. For the surface wetting properties, apparent contact angle measurements were performed with three liquids of different surface tension (γL): water γL = 72.8 mN/m, diiodomethane γL = 50.8 mN/m and hexadecane γL = 27.6 mN/m.

3. Results and Discussion

All monomers were electropolymerized by soft-template electropolymerization. In order to determine the effect of H_2O in the formation of porous structures, two solvents were used CH_2Cl_2 and CH_2Cl_2 + H_2O sat. The monomers having oxidation potential (E^{ox}) close to 2 V *vs* SCE, they were electrodeposited by cyclic voltammetry from -1 V to E^{ox} in order to have also H_2O reduction at around -0.5 V ($2H_2O + 2e^- \rightarrow H_2 + 2OH^-$) and as a consequence release of H_2 bubbles. Examples of cyclic voltammograms are given on Figure 1. All the monomers give polymer films even if non-polymerizable substituents are used such as NaphDOT-OH, NaphDOT-Ph or NaphDOT-Phen, that means only dimers are formed as represented in Scheme 3.

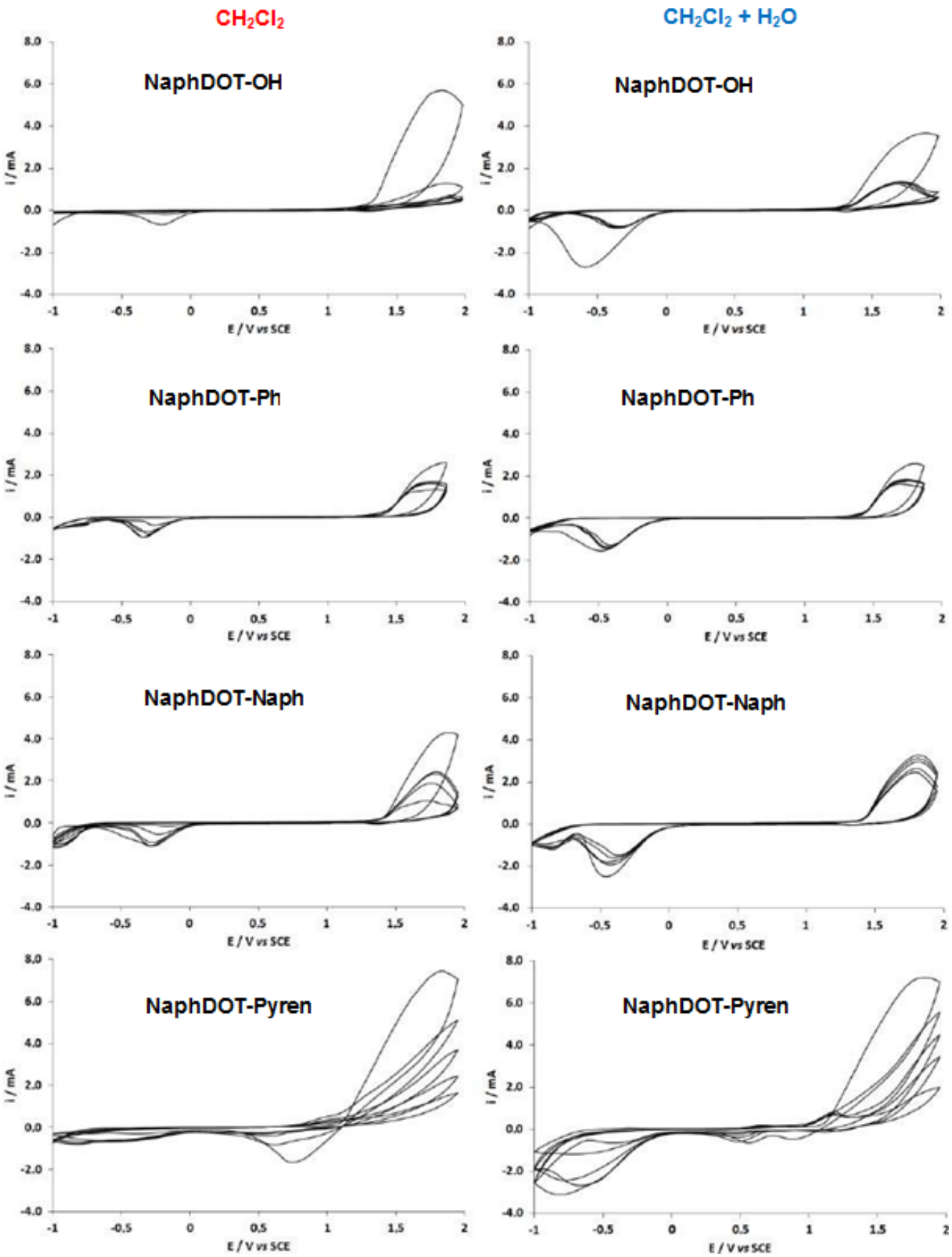

Figure 1. *Examples of cyclic voltammogram in CH_2Cl_2 and CH_2Cl_2 + H_2O. The monomer concentration was 0.01 M, the electrolyte Bu_4NClO_4 was 0.1 M, the potential range between -1 V and E^{ox}, and the scan rate 10 mV s^{-1}. The number of scan was five.*

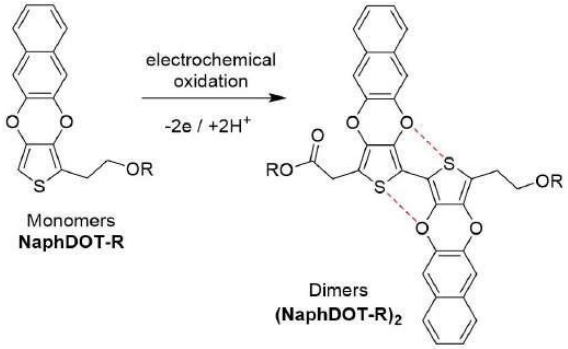

Scheme 3. *Electrochemical dimerization of 2-subtituted NaphDOT monomers. Red dashed line shows attractive S ··O contacts which planarize the dimers (NaphDOT-R)2.*

Then, the polymer films were investigated by cyclic voltammetry in free-monomer solution. In most of the CV curves of the electrodeposited polymer films (Figure 2), there is only one oxidation and reduction peak confirming that the substituent does not highly participate to the polymerization. A peak of low intensity is observed with phenyl, pyrrole and carbazole substituents. By contrast, a huge peak is present with a pyrene substituent at around 1 V *vs* SCE in a typical region for CV response of electrochemically prepared pyrene polymers.

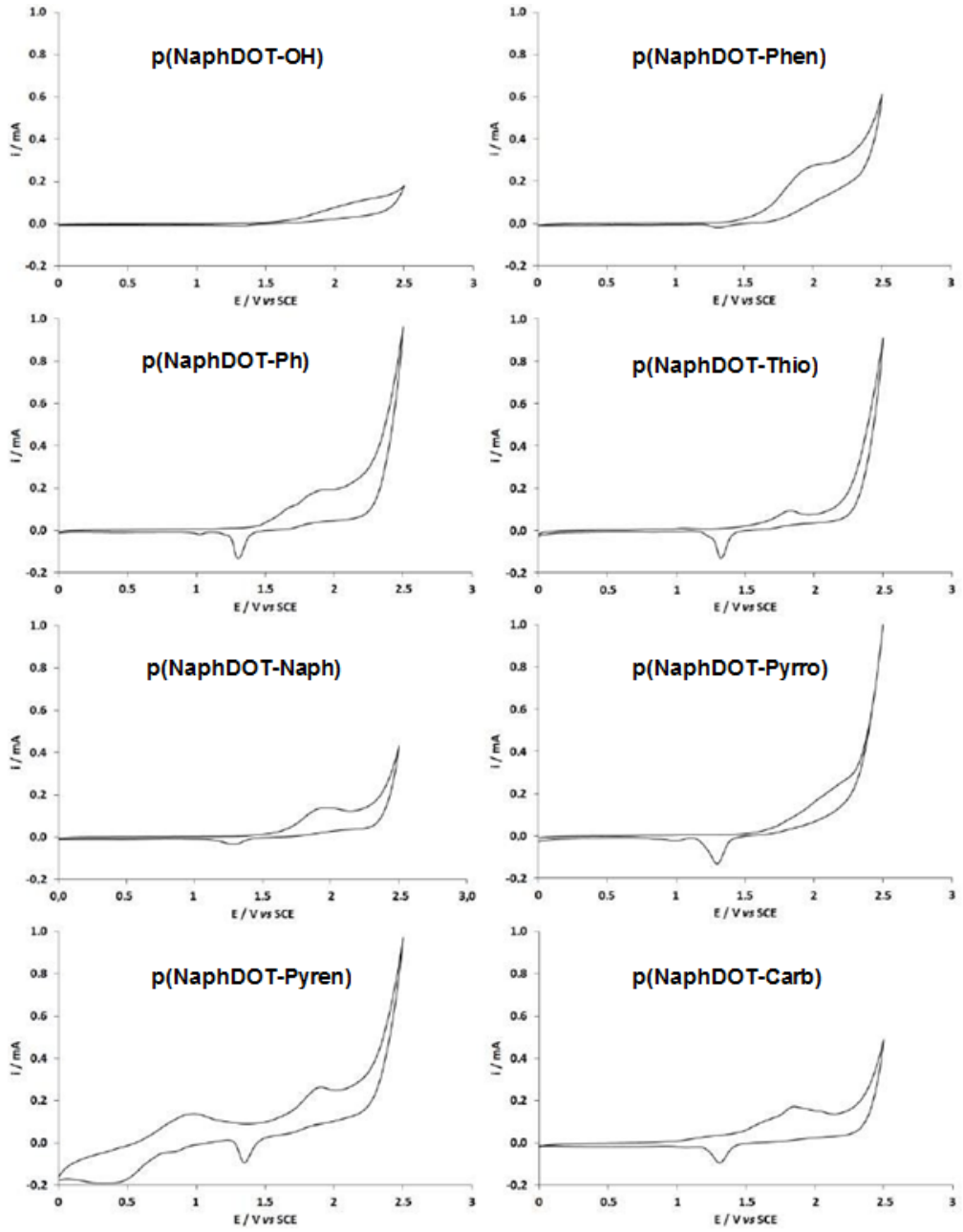

Figure 2. *Cyclic voltammograms of the electrodeposited films in CH_2Cl_2. The electrolyte Bu4NClO4 was 0.1 M, the potential range between 0 V and 2.5 V, and the scan rate 10 mV s^{-1}. The number of scan was one.*

The different surface structures are gathered in Figure 3 and Figure 4. The SEM analyses show first that the surfaces obtained in CH2Cl2 are relatively smooth. The surface obtained from NaphDOT-Pyren has non-porous spherical particles and from NaphDOT-Thio some tubular structures. In $CH_2Cl_2 + H_2O$, a huge number of nanotubes of very small size are observed especially with NaphDOT-OH and NaphDOT-Pyrro. Unique results are obtained with NaphDOT-Pyren, which leads to very huge open structures. These results can be explained by π-stacking interactions known between pyrene moieties, and the participation to polymerization.

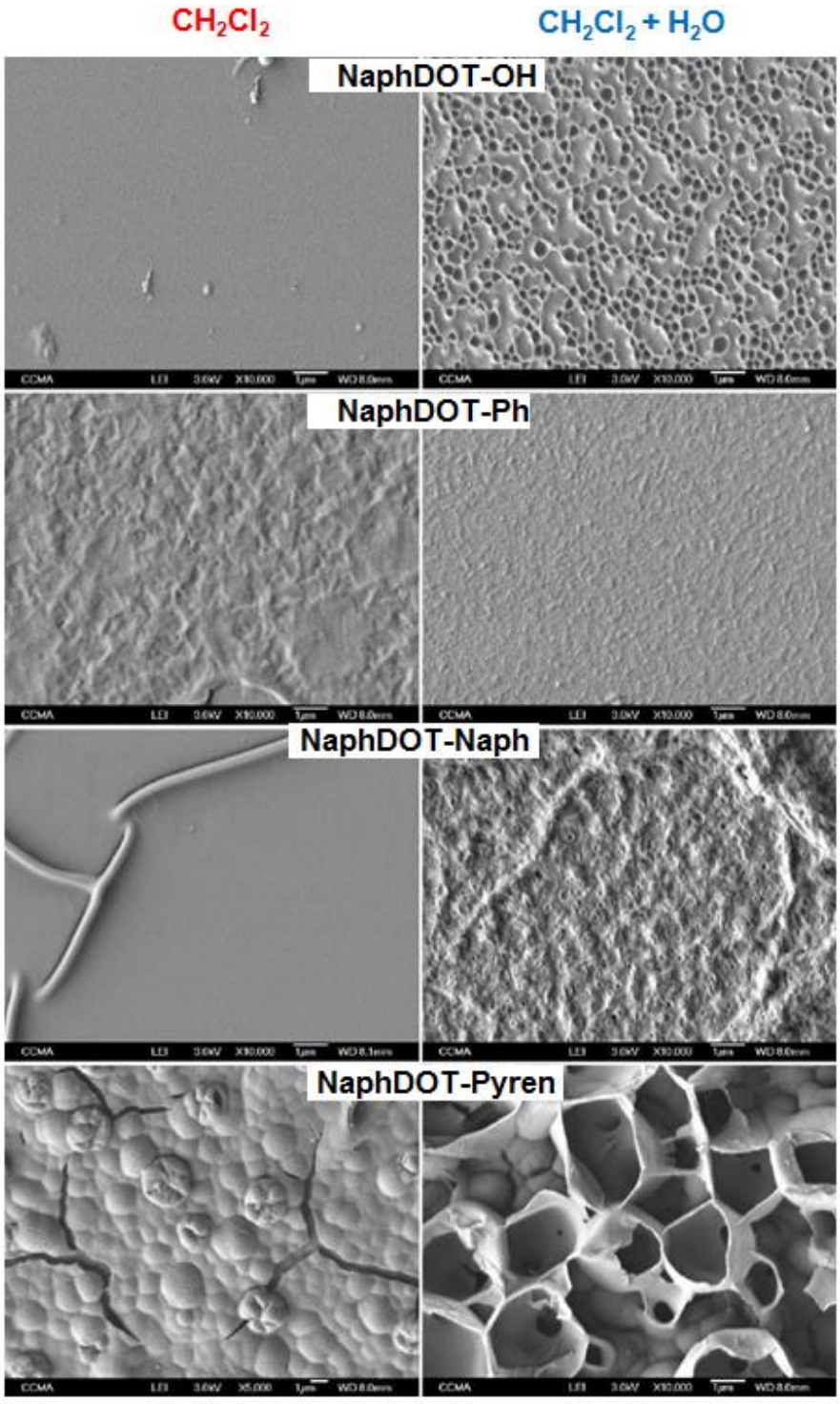

Figure 3. *SEM images of the electrodeposited films from NaphDOT-OH, NaphDOT-Ph, NaphDOT-Naph and NaphDOT-Pyren in CH2Cl2 and CH2Cl2 + H2O. The electrolyte Bu4NClO4 was 0.1 M, the potential range between -1 V and* E^{ox}*, and the scan rate 10 mV* s^{-1}*. The number of scan was three.*

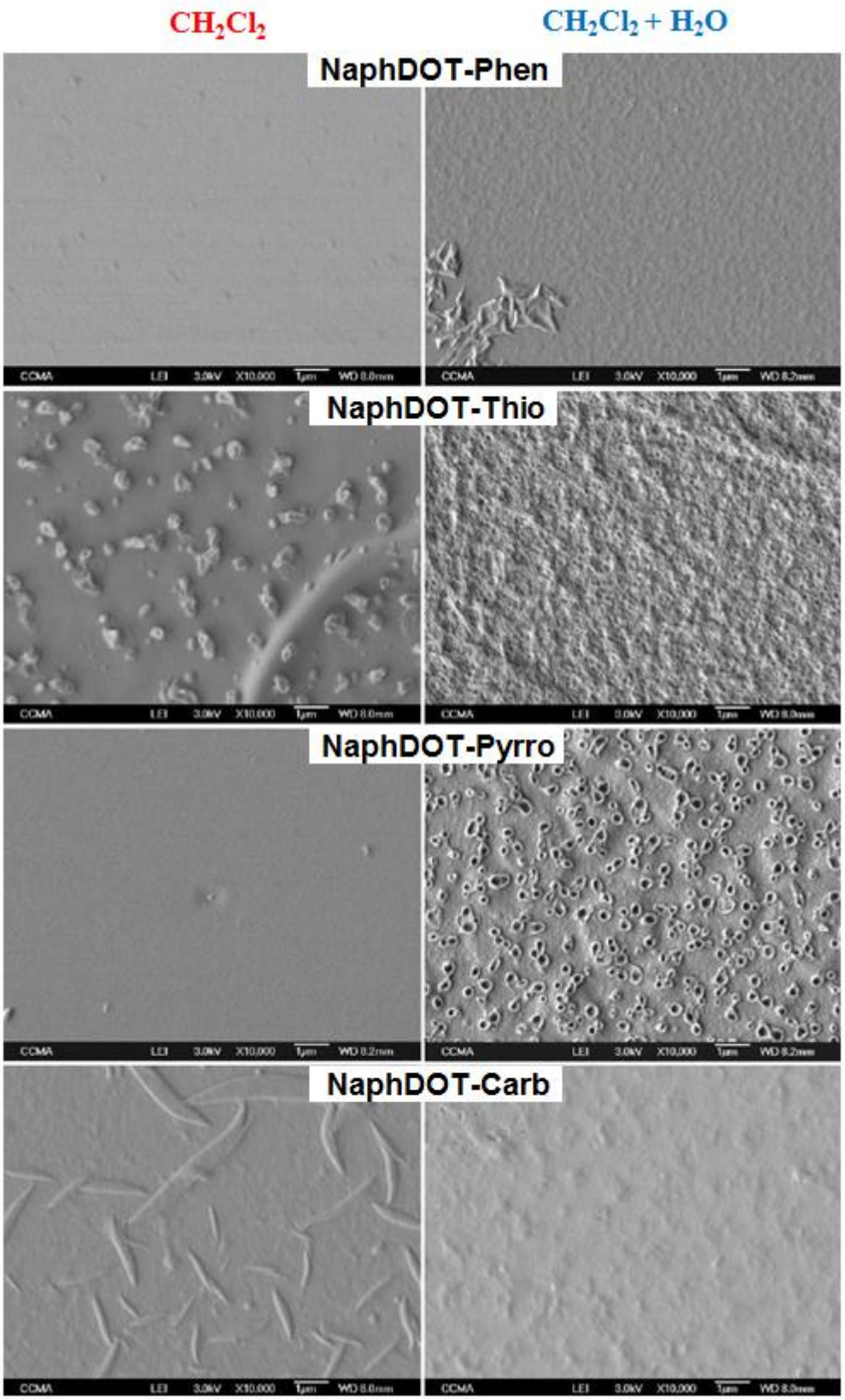

Figure 4. *SEM images of the electrodeposited films from NaphDOT-Phen, NaphDOT-Thio, NaphDOT-Pyrro and NaphDOT-Carb in CH_2Cl_2 and $CH_2Cl_2 + H_2O$. The electrolyte Bu_4NClO_4 was 0.1 M, the potential range between -1 V and E^{ox}, and the scan rate 10 mV s^{-1}. The number of scan was three.*

The surface wettability was evaluated by measuring apparent contact angles (θ) with three liquids of very different surface tension: water (γL = 72.8 mN/m) to demonstrate the hydrophobicity and diiodomethane (γL =50.0 mN/m) and hexadecane (γL =

27.6 mN/m) for the oleophobicity. The results are gathered in Table 1. The surface roughness was also determined by optical profilometry (Table 2). These data are just for information because there is direct relationship between these values and the contact angles.

Table 1. *Wettability data with water, diiodomethane and hexadecane for the polymer films obtained by cyclic voltammetry in in 0.1 M Bu_4NClO_4 / CH_2Cl_2 or CH_2Cl_2 + H_2O in potentiodynamic conditions by cyclic voltammetry (E = –1 / +E^{ox} V).*

Monomer	Number of CV Scans	θw [deg] CH_2Cl_2	θw [deg] CH_2Cl_2+H_2O	θdiiodo [deg] CH_2Cl_2	θdiiodo [deg] CH_2Cl_2+H_2O	θhexa [deg] CH_2Cl_2	θhexa [deg] CH_2Cl_2+H_2O
NaphDOT-OH	1	91.3	98.1	<10	<10	<10	<10
	3	90.3	117.7	<10	<10	<10	<10
	5	86.1	102.7	<10	<10	<10	<10
NaphDOT-Ph	1	48.6	51.3	55.0	45.3	36.5	<10
	3	40.4	52.9	45.0	44.8	12.9	12.6
	5	44.8	53.3	47.2	39.7	21.2	<10
NaphDOT-Naph	1	56.8	44.0	40.6	49.7	16.4	21.6
	3	48.3	68.0	49.0	41.8	<10	<10
	5	74.1	69.9	42.8	37.7	<10	<10
NaphDOT-Pyren	1	83.7	71.9	31.1	39.3	<10	<10
	3	79.0	92.2	24.9	39.7	<10	<10
	5	101.6	113.9	21.3	<10	<10	<10
NaphDOT-Carb	1	48.2	58.2	37.5	44.2	17.3	15.3
	3	87.1	73.7	31.6	45.5	<10	12.2
	5	64.5	69.7	44. 8	36.2	13.6	<10
NaphDOT-Thio	1	75.0	49.6	33.3	45.2	<10	14.2
	3	78.0	50.8	24.4	47.6	<10	<10
	5	65.5	76.0		30.2	<10	<10
NaphDOT-Phen	1	40.1	57.7	37.9	57.7	<10	<10
	3	62.2	72.7	39.1	72.7	<10	<10
	5	55.0	67.6	47.1	67.6	14.4	<10
NaphDOT-Pyrro	1	70.8	97.1	19.2	13.7	29.9	<10
	3	54.4	100.3	14.0	24.5	28.6	<10
	5	93.6	95.4	34.2	<10	17.9	<10

Table 2. *Arithmetic and quadratic roughness (Ra and Rq) for the polymer films obtained by cyclic voltammetry in 0.1 M Bu_4NClO_4 / CH_2Cl_2 or CH_2Cl_2 + H_2O and in potentiodynamic conditions by cyclic voltammetry (E = –1 /+E^{ox} V).*

Monomers	Solvents	CH_2Cl_2		CH_2Cl_2+H_2O	
	Number of scans	Ra [nm]	Rq [nm]	Ra [nm]	Rq [nm]
NaphDOT-OH	1	48	57	28	35

Monomers	Solvents	CH_2Cl_2		CH_2Cl_2+H_2O	
	Number of scans	Ra [nm]	Rq [nm]	Ra [nm]	Rq [nm]
	3	62	69	86	109
	5	52	62	95	136
	1	24	29	27	32
NaphDOT-Ph	3	25	31	27	32
	5	22	27	23	27
	1	53	75	38	47
NaphDOT-Naph	3	39	51	47	61
	5	66	80	80	102
	1	59	75	29	35
NaphDOT-Pyren	3	38	51	31	44
	5	25	31	57	61
	1	40	48	25	31
NaphDOT-Carb	3	38	46	23	27
	5	75	95	54	69
	1	44	53	53	62
NaphDOT-Thio	3	50	64	53	65
	5	70	93	70	89
	1	48	59	43	68
NaphDOT-Phen	3	42	48	37	41
	5	48	59	28	37
	1	29	35	46	59
NaphDOT-Pyrro	3	41	51	52	69
	5	53	6	83	88

Here, as already reported in the literature, conducting polymers with hydrophilic or aromatic groups are expected to be intrinsically hydrophilic with water Young' angle θwY< 90 °. As a consequence, if the water droplets completely wet rough surface, as described by Wenzel [34], it is excepted an increase of surface hydrophilicity that means a decrease of θw. However, sometimes it is observed a high increase of θw even above 90 ° but only for the polymer films with nanotubular structures. The highest angles are obtained after three CV scans in CH_2Cl_2 + H_2O for NaphDOT-OH (θw = 113.9°), after five CV scans in CH_2Cl_2+H_2O for NaphDOT-Pyren (θw = 117.7 °), and after three CV scans in CH_2Cl_2 + H_2O for NaphDOT-Pyrro (θw = 100.3°). These θw can be explained only with the Cassie-Baxter equation [14], demonstrating hence also the presence of air between the water droplet and these nanotubular surfaces.

After these preliminary tests, NaphDOT-OH, NaphDOT-Pyren and NaphDOT-Pyrro were selected for further experiments only in CH_2Cl_2 + H_2O but at constant potential (Figure 5 and Table 3). The surface structures obtained here are relatively similar than that previously obtained by CV even if with NaphDOT-Pyren the size of the structures is smaller. For the wetting properties, these surfaces are less hydrophobic. However, it is observed sometimes higher oleophobicity with diiodomethane than with water. This is possible when we have polymers which are both hydrophilic and oleophobic [35]. However, all the surfaces are superoleophilic with hexadecane because the surface tension of it is too low compared to the two other liquids used here.

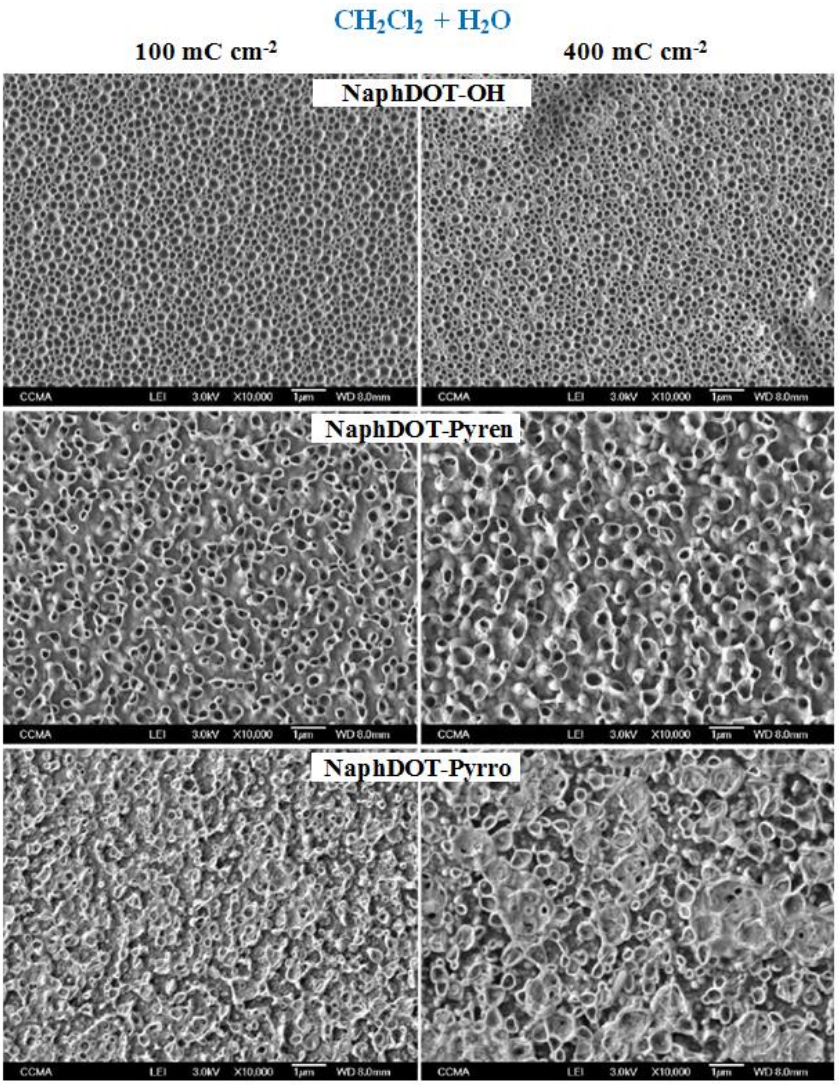

Figure 5. *SEM images of the electrodeposited films from NaphDOT-OH, NaphDOT-Pyren and NaphDOT-Pyrro in CH_2Cl_2 + H_2O. The electrolyte Bu_4NClO_4 was 0.1 M, the potential was kept constant at E^{ox}. The deposition charge was 100 and 400 mC.cm^{-2}.*

Table 3. *Wettability data with water, hexadecane and diiodomethane for the polymer films obtained by cyclic voltammetry in in 0.1 M Bu_4NClO_4 / CH2Cl2 and CH_2Cl_2 + H_2O in potentiostatic conditions at constant potential (E = +E^{ox} V).*

Monomer	Number of deposition charge [mC cm^{-2}]	θw [deg] in CH2Cl2+H2O	θdiiodo [deg] in CH2Cl2+H2O	θhexa [deg] in CH2Cl2+H2O
NaphDOT-OH	12.5	54.0	42.0	<10
	25	51.3	36.4	<10
	50	53.6	50.5	<10
	100	34.6	33.5	<10
	200	<10	38.3	<10
	400	46.1	38.5	<10
NaphDOT-Pyren	12.5	62.6	35.0	<10
	25	50.0	11.6	<10
	50	51.1	43.3	<10
	100	47.9	38.6	<10

Monomer	Number of deposition charge [mC cm^{-2}]	θw [deg] in CH2Cl2+H2O	θdiiodo [deg] in CH2Cl2+H2O	θhexa [deg] in CH2Cl2+H2O
	200	<10	34.0	<10
	400	<10	36.6	<10
NaphDOT-Pyrro	12.5	37.4	38.1	<10
	25	52.0	53.1	<10
	50	<10	40.0	<10
	100	46.0	60.7	<10
	200	63.1	64.6	<10
	400	0	60.6	<10

4. Conclusion

We demonstrated that even if dimers are formed by electropolymerization, polymer films can be obtained. NaphDOT monomers substituted at the 2-position of thiophene with various substituents were synthesized and used studied by soft template-electropolymerization. Nanotubular structures were particularly formed with hydroxyl group, pyrene and pyrrole, and in the presence of H_2O. We study also their influence on the surface hydrophobicity and found sometimes a high increase with these nanotubular structures. These surfaces could be used in the future in water-harvesting systems, for instance.

Abbreviations

γL: Surface tension Liquid
θw: Static water contact angle
Bu_4NClO_4: Tetrabutylammonium perchlorate
CDCl3: Deuterated chloroform
CH_2Cl_2: Dichloromethane
CV: Cyclic voltammetry
H_2O: Water
NaphDOT: Naphtho[2,3-b]thieno[3,4-e][1,4]dioxine
NaphDOT-Carb: 2-(naphtho[2,3-b]thieno[3,4-e][1,4]dioxin-7-yl)ethylcarbazole
NaohDOT-Naph 2-(naphtho[2,3-b]thieno[3,4-e][1,4]dioxin-7-yl)ethyl 2-naphtalenacetate
NaphDOT-OH: 2-(naphtho[2,3-b]thieno[3,4-e][1,4]dioxin-7-yl)ethanol
NaphDOT-Ph: 2-(naphtho[2,3-b]thieno[3,4-e][1,4]dioxin-7-yl)ethyl 2-phenylacetate
NaphDOT-Phen: 2-(naphtho[2,3-b]thieno[3,4-e][1,4]dioxin-7-yl)ethyl phe-noxyphenylacetate
NaphDOT-Pyr: 2-(naphtho[2,3-b]thieno[3,4-e][1,4]dioxin-7-yl)ethyl 2-pyrenacetate
NaphDOT-Pyrro: 2-(naphtho[2,3-b]thieno[3,4-e][1,4]dioxin-7-yl)ethyl 2-pyrrolate
NaphDOT-Thio: 2-(naphtho[2,3-b]thieno[3,4-e][1,4]dioxin-7-yl)ethyl 2-thiophenacetate
P1: Naphtho[2,3-b]thieno[3,4-e][1,4]dioxine
P2: 1-(naphtho[2,3-b]thieno[3,4-e][1,4]dioxin-7-yl)ethanone
P3: 2-(naphtho[2,3-b]thieno[3,4-e][1,4]dioxin-7-yl)acetate
Ra: arithmetic Roughness
Rq: quadratic Roughness
SCE: Saturated Calomel Electrode
SEM: Scanning Electron Microscopy

Author Contributions

Fatoumata Sow: Conceptualization, Formal Analysis, Methodology
Salif Sow: Conceptualization, Formal Analysis, Methodology, Software
Abdoulaye Dramé: Investigation, Resources, Supervision, Validation, Visualization, Writing – original draft, Writing – review & editing
Alioune Diouf: Formal Analysis, Visualization
Aboubacary Sene: Data curation, Visualization
Frédéric Guittard: Conceptualization, Project administration, Supervision, Validation, Visualization
Thierry Darmanin: Conceptualization, Data curation, Formal Analysis, Investigation, Methodology, Software, Validation, Visualization

Data Availability Statement

Not applicable for this manuscript.

Conflicts of Interest

The author declares no conflicts of interest.

References

[1] De Espinosa L M, Meesorn W, Moatsou D, Weder C. Bioinspired polymer systems with stimuli-responsive mechanical properties. *Chem. Rev.*, 2017, 117, 12851–12892. https://doi.org/10.1021/acs.chemrev.7b00168

[2] Ferousi C, Majer S H, Di Mucci I M, Lancaster K M. Biological and bioinspired inorganic N–N bond- forming reactions. *Chem. Rev.*, 2020, 120, 5252–5307. https://doi.org/10.1021/acs.chemrev.9b00629

[3] Palivan C G, Goers R, Najer A, Zhang X, Cara A, Meier W. Bioinspired polymer vesicles and membranes for biological and medical applications. *Chem. Soc. Rev.*, 2016, 45, 377–411. https://doi.org/10.1039/C5CS00569H

[4] Justicia J, De Cienfuegos L A, Campaña A G, Miguel D, Jakoby V, Gansäuer A, Cuerva J M. Bioinspired terpene synthesis: a radical approach. *Chem. Soc. Rev.*, 2011, 40, 3525–3537. https://doi.org/10.1039/C0CS00220H

[5] Darmanin T, Guittard F. Superhydrophobic and superoleophobic properties in nature. *Mater. Today*, 2015, 18, 273–285. https://doi.org/10.1016/j.mattod.2015.01.001

[6] Su B, Tian Y, Jiang L. Bioinspired interfaces with superwettability: From materials to chemistry. *J. Am. Chem. Soc.*, 2016, 138, 1727–1748. https://doi.org/10.1021/jacs.5b12728

[7] Liu C, Huang J X, Guo Z G, Liu W M. An integrated mesh with an anisotropic surface for unidirectional liquid manipulation. *Chem. Commun.*, 2022, 58, 9544–9547. https://doi.org/10.1039/D2CC02957J

[8] Xu X F, Zhu T X, Zheng W W, Xian C Y, Huang J Y, Chen Z, Cai W L, Zhang W Y, Lai Y K. A robust and transparent hydrogel coating for sustainable antifogging with excellent self-cleaning and self-healing ability. *Chem. Eng. J.*, 2023, 451, 137879. https://doi.org/10.1016/j.cej.2022.137879

[9] Ramachandran R, Maani N, Rayz V, Nosonovsky M. Vibrations and spatial patterns in biomimetic surfaces: Using the shark-skin effect to control blood clotting. *Phil. Trans. R. Soc. A*, 2016, 374, 20160133. https://doi.org/10.1098/rsta.2016.0133

[10] Narayanan A, Dhinojwala A, Joy A. Design principles for creating synthetic underwater adhesives. *Chem. Soc. Rev.*, 2021, 50, 13321–13345. https://doi.org/10.1039/D1CS00316J

[11] Yong J, Bai X, Yang Q, Hou X, Chen F. Filtration and removal of liquid polymers from water (polymer/water separation) by use of the underwater superpolymphobic mesh produced with a femtosecond laser. *J. Colloid Interface Sci.*, 2021, 582, 1203–1212. https://doi.org/10.1016/j.jcis.2020.09.010

[12] Marmur A. The Lotus effect: Superhydrophobicity and metastability. *Langmuir*, 2004, 20, 3517–3519. https://doi.org/10.1021/la036369u

[13] Raufaste C, Ramos Chagas G, Darmanin T, Claudet C, Guittard F, Celestini F. Superpropulsion of droplets and soft elastic solids. *Phys. Rev. Lett.*, 2017, 119, 108001. https://doi.org/10.1103/PhysRevLett.119.108001

[14] Cassie A B D, Baxter S. Wettability of porous surfaces. *Trans. Faraday Soc.*, 1944, 50, 546–551. https://doi.org/10.1039/TF9444000546

[15] Cheng Z J, Gao J, Jiang L. Tip geometry controls adhesive states of superhydrophobic surfaces. *Langmuir*, 2010, 26, 8233–8238. https://doi.org/10.1021/la904510n

[16] Ebrahimi M, Bayat A, Ardekani S R, Iranizad E S, Moshfegh A Z, Sustainable superhydrophobic branched hierarchical ZnO nanowires: Stability and wettability phase diagram. *Appl. Surf. Sci.*, 2021, 61, 150068. https://doi.org/10.1016/j.apsusc.2021.150068

[17] Li Z X, Jia M, Doble S, Hockey E, Yan H, Avenoso J P, Bodine D, Zhang Y Y, Ni C Y, Newberg J T, Gundlach L. Energy band architecture of a hierarchical ZnO/Au/CuxO nanoforest by mimicking natural superhydrophobic surfaces. *ACS Appl. Mater. Interfaces*, 2019, 11, 40490–40502. https://doi.org/10.1021/acsami.9b13610

[18] Cosnier S, Karyakin A (Eds). *Electropolymerization: Concepts, Materials and Applications*, Wiley-VCH Verlag GmbH & Co. KGaA, 2010, https://doi.org/10.1002/9783527630592

[19] Lin H A, Luo S C, Zhu B, Chen C, Yamashita Y, Yu H h. Molecular or nanoscale structures? The deciding factor of surface properties on functionalized poly(3,4-ethylenedioxythiophene) nanorod arrays. *Adv. Funct. Mater.*, 2013, 23, 3212–3219. https://doi.org/10.1002/adfm.201203006

[20] Liu L, Zhao C J, Zhao Y M, Jia N Q, Zhou Q, Yan M M, Jiang Z Y. Characteristics of polypyrrole (PPy) nano-tubules made by templated ac electropolymerization. *Eur. Polym. J.*, 2005, 41, 2117–2121. https://doi.org/10.1016/j.eurpolymj.2005.03.025

[21] Liu X L, Xu F Q, Li Z M, Zhu J F, Zhang W H. Synthesis and optical properties of poly[3-(2-methoxyphenyl)thiophene] nanowires confined in porous anodic alumina membrane. Opt. Mater., 2008, 30, 1861–1866. https://doi.org/10.1016/j.optmat.2007.12.008

[22] Fakhry A, Cachet H, Debiemme-Chouvy C. Mechanism of formation of templateless electrogenerated polypyrrole nanostructures. *Electrochim. Acta*, 2015, 179, 297–303. https://doi.org/10.1016/j.electacta.2015.03.025

[23] Qu L T, Shi G Q, Chen F, Zhang J X. Electrochemical growth of polypyrrole microcontainers. *Macromolecules*, 2003, 36, 1063–1067. https://doi.org/10.1021/ma021177b

[24] Sane O, Diouf A, Morán Cruz G, Savina F, Méallet-Renault R, Amigoni S, Dieng S Y, Guittard F, Darmanin T. Coral-like nanostructures. *Mater. Today*, 2019, 31, 119–120. https://doi.org/10.1016/j.mattod.2019.09.020

[25] Darmanin T, Bombera R, Colpo P, Valsesia A, Laugier J P, Rossi F, Guittard F. Bioinspired rose petal-like substrates generated by electropolymerization on micropatterned gold substrates. *ChemPlusChem*, 2017, 82, 352–357. https://doi.org/10.1002/cplu.201600387

[26] Khodja M, Bousrih I, El Kateb M, Beji M, Guittard F, Darmanin T. Formation of nanotubular structures with petal effect by soft-template electropolymerization of benzotrithiophene with hydrophilic carboxyl group. J. Bionic Eng., 2022, 19, 1054–1063. https://doi.org/10.1007/s42235-022-00193-1

[27] Fradin C, Orange F, Amigoni S, Guittard F, Darmanin T. Effect of electrolyte nature on micellar soft- template electropolymerization in organic solvent to form nanoporous polymer films with a bioinspired strategy. *J. Bionic Eng.*, 2022, 19, 547–553. https://doi.org/10.1007/s42235-021-00131-7

[28] Luo S C, Sekine J, Zhu B, Zhao H, Nakao A, Yu H h. Polydioxythiophene nanodots, nonowires, nano- networks, and tubular structures: the effect of functional groups and temperature in template-free electropolymerization. *ACS Nano*, 2021, 6, 3018–3026. https://doi.org/10.1021/nn300737e

[29] Darmanin T, Guittard F. A one-step electrodeposition of homogeneous and vertically aligned nanotubes with parahydrophobic properties (high water adhesion). *J. Mater. Chem. A*, 2016, 4, 3197–3203. https://doi.org/10.1039/C5TA09253A

[30] Fradin C, Orange F, Amigoni S, Szczepanski C R, Guittard F, Darmanin T. Micellar formation by soft template electropolymerization in organic solvents. *J. Colloid Interface Sci.*, 2021, 590, 260–267. https://doi.org/10.1016/j.jcis.2021.01.038

[31] Fradin C, Guittard F, Perepichka I F, Darmanin T. Soft-template electropolymerization of 3,4-(2,3- naphtylenedioxy)thiophene-2-acetic acid esters favoring dimers: Controlling the surface nanostructure by side ester groups. *Electrochim. Acta*, 2022, 425, 140684. https://doi.org/10.1016/j.electacta.2022.140684

[32] Poverenov E, Sheynin Y, Zamoshchik N, Patra A, Leitus G, Perepichka I F, Bendikov M. Flat conjugated polymers combining a relatively low HOMO energy level and band gap: Polyselenophenes versus polythiophenes. *J. Mater. Chem.*, 2012, 22, 14645–14655. https://doi.org/10.1039/C2JM31035J

[33] McKillop A, Swann B P, Taylor E C. Thallium in organic synthesis. XXXIII. A onestep synthesis of methyl arylacetates from acetophenones using thallium(III) nitrate (TTN). *J. Am. Chem. Soc.*, 1973, 95, 3340–3343. https://doi.org/10.1021/ja00791a043

[34] Wenzel R W. Resistance of solid surfaces to wetting by water. *Ind. Eng. Chem.*, 1936, 28, 988–994. https://doi.org/10.1021/ie50320a024

[35] Wang Y J, Gong X. Special oleophobic and hydrophilic surfaces: Approaches, mechanisms, and applications, *J. Mater. Chem. A*, 2017, 5, 3759–3773. https://doi.org/10.1039/C6TA10474F